

Metal-to-Ligand Charge Transfer in the Gas-Phase Cluster Limit

Thomas G. Spence,[†] Brett T. Trotter, Thomas D. Burns,[‡] and Lynmarie A. Posey*

Department of Chemistry, Vanderbilt University, Box 1822, Station B, Nashville, Tennessee 37235

Received: May 20, 1998

The solvent dependence of metal-to-ligand charge transfer (MLCT) in the bis(2,2',2''-terpyridyl)iron(II) complex, $[\text{Fe}(\text{terpy})_2]^{2+}$, isolated in small gas-phase clusters with one or four molecules of the polar, organic solvents acetone, acetonitrile, dimethyl sulfoxide, *N,N*-dimethylformamide, methanol, and pyridazine is reported. The shift in the maximum of the MLCT band, E_{op} , for $[\text{Fe}(\text{terpy})_2 \cdot (\text{solvent})_n]^{2+}$ clusters, measured using laser photofragmentation mass spectrometry, relative to the corresponding values in bulk solution ranges from $+601 \text{ cm}^{-1}$ for acetone to $+764 \text{ cm}^{-1}$ for pyridazine. The solvent dependence of the outer-sphere reorganization energy predicted by a dielectric continuum model provides a context for comparing E_{op} values determined for MLCT in $[\text{Fe}(\text{terpy})_2 \cdot (\text{solvent})_n]^{2+}$ clusters ($n = 1, 4$) with those measured in solution. A model derived from Kirkwood's equation for the mutual electrostatic interaction energy of an ion and a polar medium predicts that the solvent reorganization energy associated with MLCT in $[\text{Fe}(\text{terpy})_2]^{2+}$ is a linear function of $(1 - D_{\text{op}})/(2D_{\text{op}} + 1)$, where D_{op} is the optical dielectric constant of the bulk solvent. A linear relationship between E_{op} and $(1 - D_{\text{op}})/(2D_{\text{op}} + 1)$ is observed not only in the bulk solvents, as anticipated, but also in clusters containing as few as four solvent molecules.

I. Introduction

In solution, the energy of an optical transition to prepare a charge-transfer excited state, E_{op} , consists of contributions from the zero-point energy difference between the ground and excited states, ΔE_{o} , inner-sphere reorganization, E_{in} , and outer-sphere (solvent) reorganization, E_{out} .¹ Generally, these contributions are considered separable, and in this limit

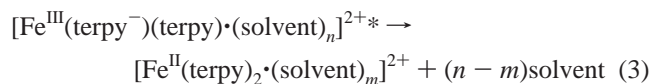
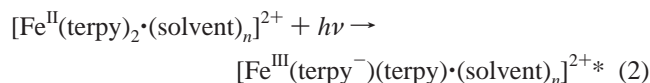
$$E_{\text{op}} = \Delta E_{\text{o}} + E_{\text{in}} + E_{\text{out}} \quad (1)$$

Alternatively, E_{op} , which corresponds to the maximum of the charge-transfer (CT) absorption band, can be broken down into components corresponding to the energy of the CT transition in the isolated gas-phase chromophore and the energy resulting from differential solvation of the ground and excited states of the chromophore. In this approach, the energy of the CT transition in the isolated chromophore is equivalent to $\Delta E_{\text{o}} + E_{\text{in}}$, and the differential solvation energy corresponds to the solvent reorganization energy, E_{out} . Conceptually, the investigation described in this paper is based upon the latter approach of separating the CT energy into gas-phase and solution components; gas-phase clusters are employed to study the influence of solvent on the energy of the metal-to-ligand charge-transfer (MLCT) transition in the coordination complex bis(2,2',2''-terpyridyl)iron(II), $[\text{Fe}(\text{terpy})_2]^{2+}$.

In principle, it should be straightforward to determine the bulk solvent reorganization energy associated with CT by taking the difference between the values of E_{op} measured for the coordination complex in solution and in the gas phase. However, it is difficult to transfer nonvolatile, multiply charged

coordination complexes, such as $[\text{Fe}(\text{terpy})_2]^{2+}$, to the gas phase while avoiding reduction^{2–4} in order to measure E_{op} for the isolated complex. Although this problem can be overcome with electrospray ionization (ESI),^{5–8} the concentrations of the gas-phase ions produced preclude direct absorption measurements. Furthermore, measurement of E_{op} for the isolated complex and comparison with the solution value provide no information on the contributions of individual solvent molecules to the bulk solvent reorganization energy. The ESI process, which transfers ionic coordination complexes^{9,10} and organometallic compounds^{11–13} to the gas phase, can also be exploited to prepare clusters of these complexes with solvent.^{7,8,14} These clusters can then be probed using laser photofragmentation mass spectrometry,^{15,16} which not only enables detection of absorption by the complex but also allows measurement of the contributions of individual solvent molecules to the reorganization energy associated with charge transfer.

This paper reports the solvent dependence of E_{op} for the MLCT transition in small $[\text{Fe}(\text{terpy})_2 \cdot (\text{solvent})_n]^{2+}$ clusters ($n = 1, 4$) determined from photodepletion action spectra collected using laser photofragmentation mass spectrometry. Excitation of the $d \rightarrow \pi^*$ transition from the 1A_1 ground state to the lowest $^1\text{MLCT}$ excited state in the low-spin¹⁷ $[\text{Fe}(\text{terpy})_2]^{2+}$ complex results in evaporation of solvent molecules from these clusters:



Rapid intersystem crossing from the $^1\text{MLCT}_1$ state ($\tau < 1 \text{ ps}$) to the long-lived 5T_2 ligand-field excited state ($\tau = 2.54 \pm 0.13 \text{ ns}$ in water)¹⁸ prevents the initially prepared $^1\text{MLCT}_1$ excited state from emitting fluorescence,¹⁹ creating an ideal situation for detection of absorption via cluster photofragmentation.

* To whom correspondence should be addressed. E-mail: lynmarie.a.posey@vanderbilt.edu.

[†] Current address: Department of Chemistry, Stanford University, Stanford, CA 94305.

[‡] Current address: Department of Chemistry, Florida Southern College, Lakeland, FL 33801.

The influence of solvent on the energetics of photoinitiated charge transfer in coordination complexes typically has been studied in the condensed phase by measuring E_{op} in different solvents and then correlating the behavior of E_{op} with functions of the static and optical dielectric constants, D_s and D_{op} .^{20–24} Any deviations^{25–30} in E_{op} from the dependence on bulk dielectric constants predicted by dielectric continuum models^{31–36} have been attributed to specific molecular interactions between the solvent and CT chromophore. By analogy with solution studies, E_{op} is determined as a function of solvent while keeping the number of solvent molecules in the cluster fixed in this study. However, in contrast with the corresponding solution studies, the environment surrounding the $[\text{Fe}(\text{terpy})_2]^{2+}$ complex in the gas-phase clusters studied is limited to first-shell solvent, where molecular-level interactions between the solvent and ionic chromophore are expected to have a significant impact on CT.^{22,37,38} Gas-phase clusters offer an opportunity to examine the point at which the properties of a structureless dielectric continuum take precedence over “specific” solvent–solute interactions in determining the solvent dependence of E_{op} . In this work, the values of E_{op} for MLCT determined from the photodepletion action spectra of $[\text{Fe}(\text{terpy})_2]^{2+}$ are compared with solution values within the context of a dielectric continuum model appropriate to the $[\text{Fe}(\text{terpy})_2]^{2+}$ system, which will be described subsequently.

II. Experimental Section

Bis(2,2',2''-terpyridyl)iron(II), $[\text{Fe}(\text{terpy})_2]^{2+}$, was synthesized following the procedures described by Morgan and Burstall³⁹ from $\text{FeSO}_4 \cdot 7\text{H}_2\text{O}$ (Fisher, 99%) and 2,2',2''-terpyridine (Aldrich, 98%); it was isolated as the hexafluorophosphate salt (NaPF_6 , Aldrich, 98%). UV–visible absorption spectra of $\text{Fe}(\text{terpy})_2(\text{PF}_6)_2$ in acetone, acetonitrile, dimethyl sulfoxide (DMSO), *N,N*-dimethylformamide (DMF), methanol, and pyridazine were recorded using an Hitachi U-2000 spectrophotometer.

Gas-phase $[\text{Fe}(\text{terpy})_2]^{2+}$ ions were generated by ESI of a 1.5×10^{-4} M methanolic solution (Fisher, Certified A.C.S.) of $\text{Fe}(\text{terpy})_2(\text{PF}_6)_2$. Simultaneously, with the region between the electrospray needle and the metal capillary, which serves as the sampling orifice into the tandem mass spectrometer, was gently purged by N_2 saturated with acetone, acetonitrile, DMSO, DMF, methanol, or pyridazine vapor. All solvents were Certified A.C.S. grade (Fisher) except DMF (Fisher, reagent grade) and pyridazine (Aldrich, 98%). Conditions in the source were optimized for the production of $[\text{Fe}(\text{terpy})_2 \cdot (\text{solvent})_n]^{2+}$ clusters, which form by the association of gas-phase ions and neutral solvent molecules in the ESI source following collisional desolvation of any $[\text{Fe}(\text{terpy})_2 \cdot (\text{CH}_3\text{OH})_n]^{2+}$ clusters formed directly by ESI.⁸

The tandem mass spectrometer and dye laser used to obtain photodepletion action spectra have been described in detail previously.¹⁵ A subsequent paper provides an updated description of the mass spectrometer and methods used to obtain photodepletion action spectra of mass-selected clusters.¹⁶ In the present study, the signal for mass-selected $[\text{Fe}(\text{terpy})_2 \cdot (\text{solvent})_n]^{2+}$ clusters ($n = 1, 4$) following the mass-analyzing stage of the tandem mass spectrometer ranged from 1800 to 6000 ions s^{-1} .

Cluster absorption spectra were collected by measuring photodepletion of the mass-selected cluster ions as a function of photon energy as the dye laser (Coherent 899-01, typical line width < 2 GHz) was stepped from 1.78×10^4 to 1.89×10^4 cm^{-1} (Rhodamine 560 and Pyrromethene 556 dyes, Exciton) in approximately 14 cm^{-1} increments. The dye laser was

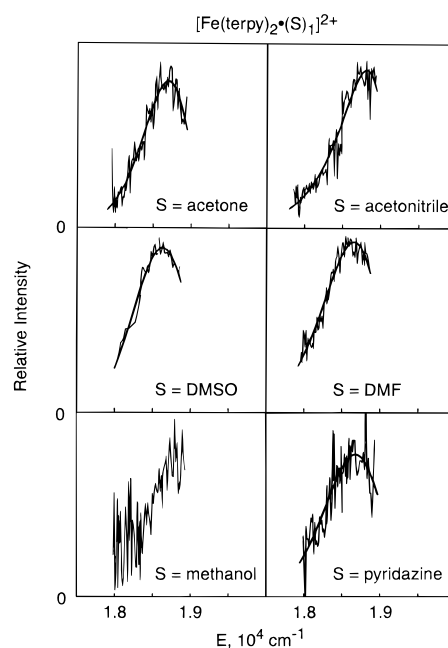


Figure 1. Photodepletion action spectra for $[\text{Fe}(\text{terpy})_2 \cdot (\text{solvent})_n]^{2+}$ clusters collected between 1.78×10^4 and 1.89×10^4 cm^{-1} (DMSO = dimethyl sulfoxide, DMF = *N,N*-dimethylformamide). The smooth lines through the data represent nonlinear least-squares fits of the data to log-normal functions.

chopped at 30 Hz, and the ion intensity was sampled for 3500 10 ms periods before average laser-on and laser-off ion intensities were recorded. Percent depletion of the ion beam was normalized with respect to laser power, which was held below 400 mW (91 W cm^{-2}) to avoid saturation of the strong MLCT transition. At each photon energy in a scan, 3–5 individual determinations of the percent depletion were made. The photodepletion action spectra reported are composites of 3–5 scans through each spectral region. The data were averaged when the photon energies for scans through the same spectral region coincided; otherwise, the individual data points were plotted. As a consequence, the data density in many cases is greater than one point per 14 cm^{-1} , the step size on individual scans. Scans obtained for a particular cluster on different days or using different laser dyes were normalized using overlapping data points to correct for changes in laser and ion beam overlap.

III. Results

Figure 1 shows the photodepletion action spectra collected from 1.78×10^4 to 1.89×10^4 cm^{-1} for $[\text{Fe}(\text{terpy})_2 \cdot (\text{solvent})_n]^{2+}$ clusters, where solvent = acetone, acetonitrile, DMSO, DMF, methanol, and pyridazine; the photodepletion action spectra for clusters containing four solvent molecules, $[\text{Fe}(\text{terpy})_2 \cdot (\text{solvent})_4]^{2+}$, appear in Figure 2. These photodepletion action spectra track the transition that promotes an electron from a metal-centered e orbital (D_{2d} symmetry) in $[\text{Fe}(\text{terpy})_2]^{2+}$ to the lowest of the ligand-based π^* orbitals⁴⁰ because the ${}^1\text{MLCT}_1$ excited state decays exclusively by nonradiative pathways.^{18,19} A detailed discussion of the spectroscopy and structure of the $[\text{Fe}(\text{terpy})_2]^{2+}$ complex is provided elsewhere.¹⁶ The smooth lines through the data are nonlinear least-squares fits of the data to a log-normal line shape.^{16,41} The band maximum for each $[\text{Fe}(\text{terpy})_2 \cdot (\text{solvent})_n]^{2+}$ cluster ($n = 1, 4$) is reported in Table 1 along with the corresponding MLCT band maximum in bulk solution ($n \rightarrow \infty$). The spectrum obtained for $[\text{Fe}(\text{terpy})_2 \cdot (\text{methanol})_4]^{2+}$ clusters was not fit to a log-normal line shape due to the absence of a single, clearly defined maximum. There

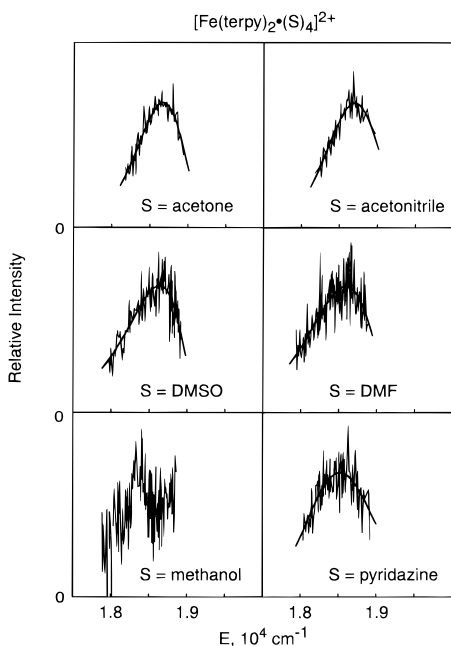


Figure 2. Photodepletion action spectra for $[\text{Fe}(\text{terpy})_2 \cdot (\text{solvent})_4]^{2+}$ clusters collected between 1.78×10^4 and $1.89 \times 10^4 \text{ cm}^{-1}$ (DMSO = dimethyl sulfoxide, DMF = *N,N*-dimethylformamide). The smooth lines through the data represent nonlinear least-squares fits of the data to log-normal functions.

appears to be a band maximum at $(1.83\text{--}1.84) \times 10^4 \text{ cm}^{-1}$ in the spectrum of $[\text{Fe}(\text{terpy})_2 \cdot (\text{methanol})_4]^{2+}$ and possibly a second band growing in on the blue edge of the data collection window ($(1.78\text{--}1.89) \times 10^4 \text{ cm}^{-1}$). Unfortunately, the presence of a second band cannot be confirmed because the 514.5 nm line in the multiline output of the argon ion pump laser suppresses the output of the dye laser at photon energies above $1.89 \times 10^4 \text{ cm}^{-1}$.^{15,16} The capacity of methanol to form strong hydrogen bonds with itself via the hydroxyl group distinguishes it from the other polar solvents used in this study and may be responsible for the marked difference in the character of the $[\text{Fe}(\text{terpy})_2 \cdot (\text{methanol})_4]^{2+}$ spectrum. Competition between hydrogen bond formation within the solvent portion of the cluster and orientation of the solvent dipoles relative to the $[\text{Fe}(\text{terpy})_2]^{2+}$ ion may produce $[\text{Fe}(\text{terpy})_2 \cdot (\text{methanol})_4]^{2+}$ isomers in which the extent of interaction between solvent and the CT chromophore varies. The presence of isomeric forms of $[\text{Fe}(\text{terpy})_2 \cdot (\text{methanol})_4]^{2+}$ in the mass-selected ion beam is expected to result in broadening of the MLCT spectrum or even the appearance of distinguishable bands for the two isomers. Clearly, further investigation of the $[\text{Fe}(\text{terpy})_2]^{2+}$ CT chromophore isolated in different size methanol clusters and in clusters of other hydrogen-bonding solvents could provide valuable insight on this issue.

The shift of the ${}^1\text{MLCT}_1 \leftarrow {}^1\text{A}_1$ absorption bands in $[\text{Fe}(\text{terpy})_2 \cdot (\text{solvent})_n]^{2+}$ clusters ($n = 1, 4$) to the blue of their bulk solution counterparts is consistent with preferential solvation of the polar excited state relative to the nonpolar ground state of $[\text{Fe}(\text{terpy})_2]^{2+}$ by polar solvents. In $[\text{Fe}(\text{terpy})_2 \cdot (\text{solvent})_1]^{2+}$ clusters, the shift in E_{op} relative to the value in bulk solution ranges from $+601 \text{ cm}^{-1}$ for acetone to $+764 \text{ cm}^{-1}$ for pyridazine. The maximum of this MLCT band in $[\text{Fe}(\text{terpy})_2 \cdot (\text{acetonitrile})_1]^{2+}$ and $[\text{Fe}(\text{terpy})_2 \cdot (\text{methanol})_1]^{2+}$ clusters shifts nearly to or just beyond the upper limit of the data collection window dictated by our laser system. Limited data on the high-energy side of the apparent maximum for $[\text{Fe}(\text{terpy})_2 \cdot (\text{acetonitrile})_1]^{2+}$ clusters introduce uncertainty in fitting of the

data to the log-normal function to locate the band maximum and yield artificially narrow fitted line shapes. No attempt is made to fit the photodepletion action spectrum of $[\text{Fe}(\text{terpy})_2 \cdot (\text{methanol})_1]^{2+}$ clusters to the log-normal function because it is not clear that the maximum has been reached at photon energies below the upper limit on photon energy at $1.89 \times 10^4 \text{ cm}^{-1}$. As a consequence, we can only report that E_{op} for $[\text{Fe}(\text{terpy})_2 \cdot (\text{methanol})_1]^{2+}$ is greater than $1.88 \times 10^4 \text{ cm}^{-1}$ with any certainty.

Comparison of E_{op} for the $n = 1$ and $n = 4$ clusters with the same solvent allows determination of the average solvent reorganization energy associated with the second through fourth solvent molecule added to the cluster. For DMSO, E_{op} is essentially unchanged between $n = 1$ and $n = 4$, where there is only a -2 cm^{-1} shift. In fact, we found in a related study¹⁶ of $[\text{Fe}(\text{terpy})_2 \cdot (\text{DMSO})_n]^{2+}$ clusters ($n = 1\text{--}11$) that there was little change in E_{op} for $n = 1\text{--}5$. The largest shift observed between $n = 1$ and $n = 4$ was -167 cm^{-1} for pyridazine, which is an average shift of -55.7 cm^{-1} per molecule.

IV. Discussion

In an effort to establish a connection between our gas-phase cluster studies and solution studies of MLCT, we have examined the solvent dependence of E_{op} for these small clusters containing a fixed number of solvent molecules while varying the solvent. As discussed in the Introduction, the energy of the CT transition, E_{op} (eq 1), can be separated into contributions related to the isolated CT chromophore, $\Delta E_0 + E_{\text{in}}$, and solvent reorganization, E_{out} . In the condensed phase, the contribution of solvent reorganization to E_{op} is typically examined using a dielectric continuum model for solvent, which neglects the details of the solvent's molecular structure and specific interactions with the CT chromophore. In fact, deviations from the behavior of E_{op} predicted by such a model are routinely ascribed to spatially directed specific interactions between the CT chromophore and solvent, such as hydrogen bonding^{25–27} or Lewis acid–base bonding.^{28–30}

The investigations of optical CT in mixtures of acetonitrile and DMSO carried out by the groups of Hupp^{37,38,42} and Curtis⁴³ provide some of strongest evidence for these “specific” solvent effects in the condensed phase. They found that E_{op} exhibited a more pronounced dependence on solution composition for DMSO mole fractions below 0.1 than the dielectric properties of the bulk solvent mixture in studies involving metal-to-metal CT in mixed-valence $\text{Ru}^{\text{II}}\text{--Ru}^{\text{III}}$ dimers and MLCT in Ru^{II} complexes having ammine ligands. The strong dependence of E_{op} on DMSO concentration when present as a very minor component was ascribed to preferential solvation of the CT chromophore resulting from hydrogen bond formation between the ammine ligands and the Lewis base DMSO. Hupp and co-workers^{37,38} concluded from these optical CT studies in mixed solvents that the bulk of the solvent reorganization energy arises from interactions of first-shell solvent molecules with the CT chromophore. This is consistent with our recent direct measurements of the solvent reorganization associated with MLCT in $[\text{Fe}(\text{terpy})_2 \cdot (\text{DMSO})_n]^{2+}$ as a function of cluster size, where we find that the first solvent shell contributes over 50% of the bulk solvent reorganization energy.¹⁶

Clearly, molecular-level solvent–solute interactions are anticipated to dominate CT behavior in small gas-phase clusters; however, deviations from the predictions of a dielectric continuum model can be used to explore these interactions within a reference frame common to the extensive body of CT work in the condensed phase. The dielectric continuum model most

TABLE 1: Metal-to-Ligand Charge-Transfer Band Maxima in $[\text{Fe}(\text{terpy})_2 \cdot (\text{solvent})_n]^{2+}$ Clusters

solvent	D_{op}^a	band max, cm^{-1}		
		$n = 1$	$n = 4$	$n \rightarrow \infty^b$
acetone	1.8463	$18\,701 \pm 15$	$18\,674 \pm 24$	$(1.810 \pm 0.002) \times 10^4$
acetonitrile	1.8070	$18\,816 \pm 17$	$18\,704 \pm 28$	$(1.813 \pm 0.002) \times 10^4$
dimethyl sulfoxide	2.1815	$18\,629 \pm 12$	$18\,631 \pm 40$	$(1.793 \pm 0.002) \times 10^4$
<i>N,N</i> -dimethylformamide	2.0463	$18\,657 \pm 13$	$18\,594 \pm 23$	$(1.800 \pm 0.002) \times 10^4$
methanol	1.7657	$> 1.88 \times 10^4$ ^c	$(1.83-1.84) \times 10^4$ ^d	$(1.814 \pm 0.002) \times 10^4$
pyridazine	2.3226	$18\,684 \pm 25$	$18\,517 \pm 20$	$(1.792 \pm 0.002) \times 10^4$

^a Values at 20 °C.⁴⁹ ^b Measured in solution at 20 °C. ^c There is insufficient data on the high-energy side of this feature to define a maximum. ^d Since the spectral data collected for this cluster do not exhibit a single, clearly defined maximum, no attempt was made to fit these data to a log-normal line shape function. The range of values reported corresponds to the low energy band and is estimated directly from the photodepletion action spectrum.

commonly applied to photoinitiated CT involving coordination complexes was developed by Marcus^{31–33} and Hush^{34,35} to treat intervalence (metal-to-metal) CT. In the Marcus–Hush model, the donor and acceptor sites for electron transfer are treated as nonoverlapping spheres separated by a fixed distance with the implication that charge separation between the donor and acceptor sites creates polar ground and excited states.

The Marcus–Hush model is clearly inappropriate for the $[\text{Fe}(\text{terpy})_2]^{2+}$ complex, where the ground state has no dipole moment and the metal-based donor and ligand-based acceptor orbitals for CT overlap. The long-range interactions between ground state $[\text{Fe}(\text{terpy})_2]^{2+}$ and the polar organic solvents used in this study are ion–dipole in nature. Excitation of the $d \rightarrow \pi^*$ MLCT transition creates a polar excited state, resulting in dipole–dipole interactions between the solute and solvent in addition to the essentially unchanged ion–dipole interactions experienced by the ground state. Meyer and co-workers²⁴ applied Kirkwood’s equation⁴⁴ for the mutual electrostatic energy of an ion in a polar medium to derive the following expression for the solvent reorganization energy associated with MLCT in the $[\text{Ru}(\text{bpy})_3]^{2+}$ and $[\text{Os}(\text{bpy})_3]^{2+}$ complexes, which also have a nonpolar ground state and polar MLCT excited state:

$$E_{\text{out}} = \frac{\bar{\mu}_{\text{es}}^2}{b^3} \left(\frac{1 - D_{\text{op}}}{2D_{\text{op}} + 1} \right) \quad (4)$$

where $\bar{\mu}_{\text{es}}$ is the excited-state dipole moment of the coordination complex, b is its effective radius, and D_{op} is the optical dielectric constant of the solvent medium. Combining eqs 1 and 4 yields

$$E_{\text{op}} = \Delta E_{\text{o}} + E_{\text{in}} + \frac{\bar{\mu}_{\text{es}}^2}{b^3} \left(\frac{1 - D_{\text{op}}}{2D_{\text{op}} + 1} \right) \quad (5)$$

for the energy of the optical transition.

Figure 3 shows the maxima of the MLCT band for $[\text{Fe}(\text{terpy})_2]^{2+}$ in solution and in gas-phase clusters containing one or four solvent molecules plotted as a function of $(1 - D_{\text{op}})/(2D_{\text{op}} + 1)$. A linear least-squares fit of the solution data ($R = 0.990$) yields a slope of $3.687 \times 10^3 \text{ cm}^{-1}$, which is equal to $\bar{\mu}_{\text{es}}^2/b^3$, and a y-intercept of $1.876 \times 10^4 \text{ cm}^{-1}$, which corresponds to $\Delta E_{\text{o}} + E_{\text{in}}$. The effective radius of the $[\text{Fe}(\text{terpy})_2]^{2+}$ complex is estimated to fall between 5.0 and 6.0 Å, putting the excited-state dipole moment in the range 9.57–12.6 D.¹⁶ Meyer and co-workers²⁴ reported values of 14.1 ± 6.1 and 13.3 ± 6.6 D for $[\text{Ru}(\text{bpy})_3]^{2+}$ and $[\text{Os}(\text{bpy})_3]^{2+}$, respectively, based on a similar analysis.

The y-intercept implies a value for E_{op} corresponding to the isolated $[\text{Fe}(\text{terpy})_2]^{2+}$ complex, which we can compare with the values of E_{op} obtained for $[\text{Fe}(\text{terpy})_2 \cdot (\text{solvent})_1]^{2+}$ clusters in the absence of a direct or indirect determination of absorption

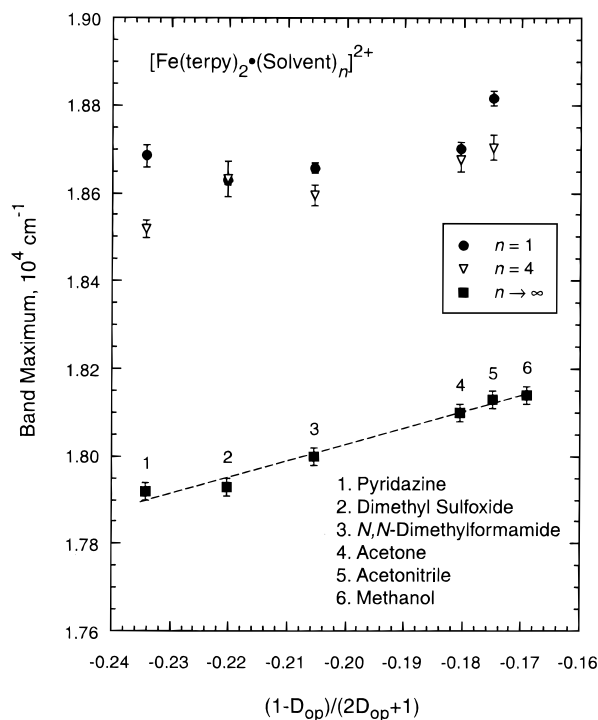


Figure 3. Metal-to-ligand charge-transfer band maxima of $[\text{Fe}(\text{terpy})_2 \cdot (\text{solvent})_n]^{2+}$ clusters ($n=1,4$) determined from photodepletion action spectra and $[\text{Fe}(\text{terpy})_2](\text{PF}_6)_2$ in bulk solution measured by UV–visible spectrophotometry plotted as a function of $(1 - D_{\text{op}})/(2D_{\text{op}} + 1)$, where D_{op} is the optical dielectric constant of the solvent.

by gas-phase $[\text{Fe}(\text{terpy})_2]^{2+}$. Electrospray ionization produces too few gas-phase $[\text{Fe}(\text{terpy})_2]^{2+}$ ions for direct absorption measurements, and the photon energies that promote MLCT fail to dissociate one of the tridentate terpyridyl ligands from the complex to permit indirect detection using laser photofragmentation mass spectrometry. The values of E_{op} for $[\text{Fe}(\text{terpy})_2 \cdot (\text{solvent})_1]^{2+}$ clusters range from $18\,629 \pm 12 \text{ cm}^{-1}$ for DMSO to $18\,816 \pm 17 \text{ cm}^{-1}$ for acetonitrile, while the values of E_{op} in DMSO and acetonitrile solutions are $(1.793 \pm 0.002) \times 10^4 \text{ cm}^{-1}$ and $(1.813 \pm 0.002) \times 10^4 \text{ cm}^{-1}$, respectively. In both cases, the energy of the MLCT transition shifts to lower energy with the addition of solvent. The higher values of E_{op} for $[\text{Fe}(\text{terpy})_2 \cdot (\text{acetonitrile})_1]^{2+}$ and $[\text{Fe}(\text{terpy})_2]^{2+}$ in acetonitrile solution relative to their DMSO counterparts indicate a weaker interaction of acetonitrile with the CT excited-state dipole moment. Hence, we conclude from the values of E_{op} determined for $[\text{Fe}(\text{terpy})_2 \cdot (\text{solvent})_1]^{2+}$ clusters that E_{op} determined for $[\text{Fe}(\text{terpy})_2 \cdot (\text{acetonitrile})_1]^{2+}$ is closest to the energy of the MLCT transition in the gas-phase $[\text{Fe}(\text{terpy})_2]^{2+}$ complex. The value of $1.876 \times 10^4 \text{ cm}^{-1}$ for $\Delta E_{\text{o}} + E_{\text{in}}$ obtained from the y-intercept of the plot of solution values for E_{op} vs $(1 - D_{\text{op}})/(2D_{\text{op}} + 1)$

provides a conservative lower limit for the MLCT transition energy in the gas-phase complex, which is within 50 cm^{-1} of the value of E_{op} for $[\text{Fe}(\text{terpy})_2(\text{acetonitrile})_1]^{2+}$.

Examination of the cluster values for E_{op} plotted as a function of $(1 - D_{\text{op}})/(2D_{\text{op}} + 1)$ reveals significant scatter in the data for the $n = 1$ clusters, which is anticipated because the bulk optical dielectric constant is not expected to apply to a situation involving a single solvent molecule. On the other hand, the $n = 4$ data for the solvents acetone, acetonitrile, DMF, and pyridazine fall on a straight line with a slope of $3.084 \times 10^3 \text{ cm}^{-1}$ and y-intercept of $1.924 \times 10^4 \text{ cm}^{-1}$ ($R = 0.996$ for linear least-squares fit), while the DMSO data for $n = 4$ fall 75 cm^{-1} above the line. Notably, E_{op} shows little size dependence in clusters containing 1–5 DMSO molecules.¹⁶ In addition, the shift from the $n = 4$ cluster to the bulk limit falls between -5.7×10^2 and $-6.0 \times 10^2 \text{ cm}^{-1}$ for the four solvents that show a linear correlation with $(1 - D_{\text{op}})/(2D_{\text{op}} + 1)$, while the shift from $n = 4$ to the bulk limit for DMSO is $-7.0 \times 10^2 \text{ cm}^{-1}$. The corresponding slope and y-intercept determined for bulk solution, considering only acetone, acetonitrile, DMF, and pyridazine, are $3.514 \times 10^3 \text{ cm}^{-1}$ and $1.874 \times 10^4 \text{ cm}^{-1}$, respectively ($R = 0.994$); these values differ only slightly from those obtained using solution data for E_{op} in all six solvents. The slope for the $[\text{Fe}(\text{terpy})_2(\text{solvent})_4]^{2+}$ cluster data is $6.0 \times 10^2 \text{ cm}^{-1}$ (12%) smaller than the bulk value, while the y-intercept is $4.8 \times 10^2 \text{ cm}^{-1}$ (2.6%) larger. Both differences are appreciable; consequently, the difference between the solvent dependence of E_{op} in bulk solution and in clusters containing four solvent molecules cannot be assigned primarily to either component of eq 5.

Despite the absence of a solvent continuum in $[\text{Fe}(\text{terpy})_2(\text{solvent})_n]^{2+}$ clusters, we observe a correlation between E_{op} and the bulk optical dielectric constant when $n = 4$. One would expect specific molecular interactions between the solvent and CT chromophore to dominate the solvent dependence of E_{op} with only four solvent molecules present. In fact, a space-filling model of $[\text{Fe}(\text{terpy})_2]^{2+}$ generated from X-ray crystallographic coordinates⁴⁵ using MacroModel⁴⁶ reveals interligand pockets with ample room to accommodate the four solvent molecules, placing the solvent molecules in close proximity to the ligands and metal center. When only one solvent molecule interacts directly with $[\text{Fe}(\text{terpy})_2]^{2+}$, the solvent dependence of E_{op} exhibits significant deviations from the predictions of a dielectric continuum model. But, by the time the fourth solvent molecule is added to clusters of $[\text{Fe}(\text{terpy})_2]^{2+}$ with acetone, acetonitrile, dimethylformamide, and pyridazine, “bulk” effects appear to override the molecular-level interactions. Further consideration of the nature of the optical dielectric constant, however, reveals that correlation of the solvent dependence of E_{op} with this bulk property in finite systems containing a fixed number of solvent molecules is not totally unreasonable. The optical dielectric constant, D_{op} , describes the response of the solvent medium to a high-frequency electric field.⁴⁷ In fact, in a dense isotropic medium $(1 - D_{\text{op}})/(2D_{\text{op}} + 1)$ is directly proportional to the number density of polarizable electrons and the polarizability of these electrons.⁴⁸ These are discrete, molecular properties of the particular solvent, which will not change appreciably with the number of solvent molecules present unless strong interactions occur between the solvent molecules.

V. Conclusions

This investigation has yielded the unexpected observation that E_{op} for MLCT in the coordination complex $[\text{Fe}(\text{terpy})_2]^{2+}$ isolated in clusters with as few as four solvent molecules shows

a solvent dependence that correlates with the behavior predicted by a dielectric continuum model. The solvent molecules should occupy the first solvent shell at such a small cluster size, and specific molecular interactions should dominate “solvation” of the CT chromophore, especially in this system where solvent molecules can sit in the interligand pockets of $[\text{Fe}(\text{terpy})_2]^{2+}$. Clearly, further study involving other charge-transfer systems is warranted. It would be particularly interesting to examine coordination complexes whose MLCT or intervalence CT transition energies in solution deviate^{25–30} from the predictions of a dielectric continuum model owing to specific interactions between solvent and the CT chromophore. The technique of coupling electrospray ionization with laser photofragmentation mass spectrometry as demonstrated here is sufficiently general that it should be possible to extend this work on the solvent dependence of photoinitiated charge transfer to other ionic coordination complexes.

Acknowledgment. Support for this work from NSF (CHE-9616606) and Research Corporation (Cottrell Scholar Award) is gratefully acknowledged. B.T.T. and L.A.P. thank Angela Anderson for assistance in the laboratory during the final stages of this work.

References and Notes

- (1) Barbara, P. F.; Meyer, T. J.; Ratner, M. A. *J. Phys. Chem.* **1996**, *100*, 13148.
- (2) Balasanmugam, K.; Day, R.; Hercules, D. M. *Inorg. Chem.* **1985**, *24*, 4477.
- (3) Beavis, R.; Lindner, J.; Grottemeyer, J.; Atkinson, I. M.; Keene, F. R.; Knight, A. E. W. *J. Am. Chem. Soc.* **1988**, *110*, 7534.
- (4) Miller, J. M.; Balasanmugam, K. *Can. J. Chem.* **1989**, *67*, 1496.
- (5) Jayaweera, P.; Blades, A. T.; Ikonomou, M. G.; Kebarle, P. *J. Am. Chem. Soc.* **1990**, *112*, 2452.
- (6) Blades, A. T.; Jayaweera, P.; Ikonomou, M. G.; Kebarle, P. *J. Chem. Phys.* **1990**, *92*, 5900.
- (7) Katta, V.; Chowdhury, S. K.; Chait, B. T. *J. Am. Chem. Soc.* **1990**, *112*, 5348.
- (8) Spence, T. G.; Burns, T. D.; Posey, L. A. *J. Phys. Chem. A* **1997**, *101*, 139.
- (9) Andersen, U. N.; McKenzie, C. J.; Bojesen, G. *Inorg. Chem.* **1995**, *34*, 1435.
- (10) Arakawa, R.; Matsuo, T.; Ito, H.; Katakuse, I.; Nozaki, K.; Ohno, T.; Haga, M. *Org. Mass Spectrom.* **1994**, *29*, 289.
- (11) Colton, R.; Traeger, J. C. *Inorg. Chim. Acta* **1992**, *201*, 153.
- (12) Kane-Maguire, L. A. P.; Kanitz, R.; Sheil, M. M. *J. Organomet. Chem.* **1995**, *486*, 243.
- (13) Hinderling, C.; Plattner, D. A.; Chen, P. *Angew. Chem., Int. Ed. Engl.* **1997**, *36*, 243.
- (14) Burns, T. D.; Spence, T. G.; Mooney, M. A.; Posey, L. A. *Chem. Phys. Lett.* **1996**, *258*, 669.
- (15) Spence, T. G.; Burns, T. D.; Guckenberger, G. B., V.; Posey, L. A. *J. Phys. Chem. A* **1997**, *101*, 1081.
- (16) Spence, T. G.; Trotter, B. T.; Posey, L. A. *J. Phys. Chem. A*, submitted.
- (17) Goodwin, H. A. *Coord. Chem. Rev.* **1976**, *18*, 293.
- (18) McCusker, J. K.; Walda, K. N.; Dunn, R. C.; Simon, J. D.; Magde, D.; Hendrickson, D. N. *J. Am. Chem. Soc.* **1993**, *115*, 298.
- (19) Fink, D. W.; Ohnesorge, W. E. *J. Am. Chem. Soc.* **1969**, *91*, 4995.
- (20) Powers, M. J.; Meyer, T. J. *J. Am. Chem. Soc.* **1978**, *100*, 4393.
- (21) Powers, M. J.; Meyer, T. J. *J. Am. Chem. Soc.* **1980**, *102*, 1289.
- (22) Sullivan, B. P.; Curtis, J. C.; Kober, E. M.; Meyer, T. J. *Nouv. J. Chim.* **1980**, *4*, 643.
- (23) Creutz, C. *Prog. Inorg. Chem.* **1983**, *30*, 1.
- (24) Kober, E. M.; Sullivan, B. P.; Meyer, T. J. *Inorg. Chem.* **1984**, *23*, 2098.
- (25) Callahan, R. W.; Meyer, T. J. *Chem. Phys. Lett.* **1976**, *39*, 82.
- (26) Callahan, R. W.; Keene, F. R.; Meyer, T. J.; Salmon, D. J. *J. Am. Chem. Soc.* **1977**, *99*, 1064.
- (27) Curtis, J. C.; Sullivan, B. P.; Meyer, T. J. *Inorg. Chem.* **1983**, *22*, 224.
- (28) Bignozzi, C. A.; Chiorboli, C.; Indelli, M. T.; Rampi Scandola, M. A.; Varani, G.; Scandola, F. *J. Am. Chem. Soc.* **1986**, *108*, 7872.
- (29) Chang, J. P.; Fung, E. Y.; Curtis, J. C. *Inorg. Chem.* **1986**, *25*, 4233.

- (30) Fung, E. Y.; Chua, A. C. M.; Curtis, J. C. *Inorg. Chem.* **1988**, *27*, 1294.
- (31) Marcus, R. A. *J. Chem. Phys.* **1956**, *24*, 966.
- (32) Marcus, R. A. *Annu. Rev. Phys. Chem.* **1964**, *15*, 155.
- (33) Marcus, R. A. *J. Chem. Phys.* **1965**, *43*, 679.
- (34) Hush, N. S. *Prog. Inorg. Chem.* **1967**, *8*, 391.
- (35) Hush, N. S. *Electrochim. Acta* **1968**, *13*, 1005.
- (36) Brunschwig, B. S.; Ehrenson, S.; Sutin, N. *J. Phys. Chem.* **1986**, *90*, 3657.
- (37) Hupp, J. T.; Weydert, J. *Inorg. Chem.* **1987**, *26*, 2657.
- (38) Blackbourn, R. L.; Hupp, J. T. *J. Phys. Chem.* **1988**, *92*, 2817.
- (39) Morgan, G.; Francis, H. B. *J. Chem. Soc.* **1937**, 1649.
- (40) Baggio-Saitovitch, E.; de Paoli, M. A. *Inorg. Chim. Acta* **1978**, *27*, 15.
- (41) Siano, D. B.; Metzler, D. E. *J. Chem. Phys.* **1969**, *51*, 1856.
- (42) Roberts, J. A.; Hupp, J. T. *Inorg. Chem.* **1992**, *31*, 157.
- (43) Ennix, K. S.; McMahon, P. T.; de la Rosa, R.; Curtis, J. C. *Inorg. Chem.* **1987**, *26*, 2660.
- (44) Kirkwood, J. G. *J. Chem. Phys.* **1934**, *2*, 351.
- (45) Baker, A. T.; Goodwin, H. A. *Aust. J. Chem.* **1985**, *38*, 207.
- (46) Mohamadi, F.; Richards, N. G. J.; Guida, W. C.; Liskamp, R.; Lipton, M.; Caufield, C.; Chang, G.; Hendrickson, T.; Still, W. C. *J. Comput. Chem.* **1990**, *11*, 440.
- (47) Cox, P. A. *The Electronic Structure and Chemistry of Solids*; Oxford University Press: New York, 1987; pp 60–62.
- (48) Davydov, A. S. *Quantum Mechanics*, 2nd ed.; Pergamon: New York, 1976; pp 424–425.
- (49) Lide, D. R. *CRC Handbook of Chemistry and Physics*, 76th ed.; CRC Press: Boca Raton, FL, 1995.